

AMUSED: AN OPEN MUSE REPRODUCTION

Suraj Patil¹, William Berman¹, Robin Rombach², Patrick von Platen¹

¹Hugging Face, ²Stability AI

{suraj, patrick}@huggingface.co

WLBberman@gmail.com

robin@stability.ai

ABSTRACT

We present aMUSEd, an open-source, lightweight masked image model (MIM) for text-to-image generation based on MUSE (Chang et al. (2023)). With 10% of MUSE’s parameters, aMUSEd is focused on fast image generation. We believe MIM is underexplored compared to latent diffusion (Rombach et al. (2022)), the prevailing approach for text-to-image generation. Compared to latent diffusion, MIM requires fewer inference steps (Chang et al. (2023)) and is more interpretable. Additionally, MIM can be fine-tuned to learn additional styles with only a single image (Sohn et al. (2023)). We hope to encourage further exploration of MIM by demonstrating its effectiveness on large-scale text-to-image generation and releasing reproducible training code. We also release checkpoints for two models which directly produce images at 256x256 and 512x512 resolutions.

1 INTRODUCTION

In recent years, diffusion based text-to-image generative models have achieved unprecedented quality (Rombach et al. (2022); Podell et al. (2023); DeepFloyd (2023); Saharia et al. (2022); Betker et al. (2023); Ramesh et al. (2022; 2021); Peebles & Xie (2023)). Improvements can be mainly attributed to large open-source pre-training datasets (Schuhmann et al. (2022a)), pre-trained text encoders (Radford et al. (2021); Raffel et al. (2023)), latent image encoding methods (Kingma & Welling (2019), Esser et al. (2021)) and improved sampling algorithms (Song et al. (2020); Zhang & Chen (2023); Lu et al. (2022a;b); Dockhorn et al. (2022); Song et al. (2021); Karras et al. (2022)).

MIM has proven to be a promising alternative to diffusion models for image generation (Chang et al. (2023; 2022)). MIM’s repeated parallel prediction of all tokens is particularly efficient for high-resolution data like images. While diffusion models usually require 20 or more sampling steps during inference, MIM allows for image generation in as few as 10 steps.

MIM brings the modeling approach closer to the well-researched field of language modeling (LM). Consequently, MIM can directly benefit from findings of the LM research community, including quantization schemes (Dettmers et al. (2022; 2023)), token sampling methods (Fan et al. (2018), Holtzman et al. (2020)), and token-based uncertainty estimation Guo et al. (2017).

As MIM’s default prediction objective mirrors in-painting, MIM demonstrates impressive zero-shot in-painting performance, whereas diffusion models generally require additional fine-tuning (RunwayML (2022)). Moreover, recent style-transfer (Sohn et al. (2023)) research has shown effective single image style transfer for MIM, but diffusion models have not exhibited the same success.

Despite MIM’s numerous benefits over diffusion-based image generation methods, its adoption has been limited. Proposed architectures require significant computational resources, e.g. MUSE uses a 4.6b parameter text-encoder, a 3b parameter base transformer, and a 1b parameter super-resolution transformer. Additionally, previous models have not released training code and modeling weights. We believe an open-source, lightweight model will support the community to further develop MIM.

In this work, we introduce *aMUSEd*, an efficient, open-source 800M million parameter model¹ based on MUSE. aMUSEd utilizes a CLIP-L/14 text encoder (Radford et al. (2021)), SDXL-style

¹Including all parameters from the U-ViT, CLIP-L/14 text encoder, and VQ-GAN.

micro-conditioning (Podell et al. (2023)), and a U-ViT backbone (Hoogeboom et al. (2023)). The U-ViT backbone eliminates the need for a super-resolution model, allowing us to successfully train a single-stage 512x512 resolution model. The design is focused on reduced complexity and reduced computational requirements to facilitate broader use and experimentation within the scientific community.

We demonstrate many advantages such as 4bit and 8bit quantization, zero-shot in-painting, and single image style transfer with styledrop (Sohn et al. (2023)). We release all relevant model weights and source code.

2 RELATED WORK

2.1 TOKEN-BASED IMAGE GENERATION

Esser et al. (2021) demonstrated the effectiveness of VQ-GAN generated image token embeddings for auto-regressive transformer based image modeling. With large-scale text-to-image datasets, auto-regressive image generation can yield state-of-the-art results in image quality (Yu et al. (2022; 2023)). Additionally, auto-regressive token prediction allows framing image and text-generation as the same task, opening an exciting research direction for grounded multimodal generative models (Huang et al. (2023); Aghajanyan et al. (2022)). While effective, auto-regressive image generation is computationally expensive. Generating a single image can require hundreds to thousands of token predictions.

As images are not inherently sequential, Chang et al. (2022) proposed MIM. MIM predicts all masked image tokens in parallel for a fixed number of inference steps. On each step, a predetermined percentage of the most confident predictions are fixed, and all other tokens are re-masked. MIM’s training objective mirrors BERT’s training objective (Devlin et al. (2018)). However, MIM uses a varied masking ratio to support iterative sampling starting from only masked tokens.

Consequently, MUSE successfully applied MIM to large-scale text-to-image generation (Chang et al. (2023)). MUSE uses a VQ-GAN (Esser et al. (2021)) with a fine-tuned decoder, a 3 billion parameter transformer, and a 1 billion parameter super-resolution transformer. Additionally, MUSE is conditioned on text embeddings from the pre-trained T5-XXL text encoder (Raffel et al. (2023)). To improve image quality when predicting 512x512 resolution images, MUSE uses a super-resolution model conditioned on predicted tokens from a 256x256 resolution model. As MIM’s default prediction objective mirrors in-painting, MUSE demonstrates impressive zero-shot in-painting results. In contrast, diffusion models generally require additional fine-tuning for in-painting (RunwayML (2022)).

MIM has not been adopted by the research community to the same degree as diffusion models. We believe this is mainly due to a lack of lightweight, open-sourced models, e.g. MUSE is closed source and has a 4.5 billion parameter text encoder, a 3 billion parameter base model, and a 1 billion parameter super-resolution model.

2.2 FEW-STEP DIFFUSION MODELS

Diffusion models are currently the prevailing modeling approach for text-to-image generation. Diffusion models are trained to remove noise from a target image at incrementally decreasing levels of noise. Models are frequently trained on 1000 noise levels (Rombach et al. (2022); Podell et al. (2023); Saharia et al. (2022); Chen et al. (2023)), but noise levels can be skipped or approximated without suffering a significant loss in image quality (Song et al. (2021); Karras et al. (2022); Song et al. (2020); Zhang & Chen (2023); Lu et al. (2022a;b); Dockhorn et al. (2022)). As of writing this report, effective denoising strategies (Lu et al. (2022b); Zhao et al. (2023); Zheng et al. (2023)) require as few as 20 steps to generate images with little to indistinguishable quality degradation compared to denoising at each trained noise level.

20 sampling steps is still prohibitively expensive for real-time image generation. Diffusion models can be further distilled to sample in as few as 1 to 4 sampling steps. Salimans & Ho (2022) shows how a pre-trained diffusion model can be distilled to sample in half the number of sampling steps. This distillation can be repeated multiple times to produce a model that requires as few as 2 to

4 sampling steps. Additionally, framing the denoising process as a deterministic ODE integration, consistency models can learn to directly predict the same fully denoised image from any intermediate noisy image on the ODE trajectory (Song et al. (2021)). Luo et al. (2023a) and Luo et al. (2023b) were the first to successfully apply consistency distillation to large-scale text-to-image datasets, generating high-quality images in as few as 4 inference steps. Sauer et al. (2023) demonstrated that an adversarial loss objective and a score distillation sampling (Poole et al. (2022)) objective can be combined to distill few step sampling.

Distilled diffusion models are faster than the current fastest MIM models. However, distilled diffusion models require a powerful teacher model. A teacher model requires additional training complexity, additional training memory, and limits the image quality of the distilled model. MIM’s training objective does not require a teacher model or approximate inference algorithm and is fundamentally designed to require fewer sampling steps.

2.3 INTERPRETABILITY OF TEXT-TO-IMAGE MODELS

Auto-regressive image modeling and MIM output explicit token probabilities, which naturally measure prediction confidence (Guo et al. (2017)). Token probability-based language models have been used to research model interpretability (Jiang et al. (2021)). We do not extensively explore the interpretability of token prediction-based image models, but we believe this is an interesting future research direction.

3 METHOD

VQ-GAN We trained a 146M parameter VQ-GAN (Esser et al. (2021)) with no self-attention layers, a vocab size of 8192, and a latent dimension of 64. Our VQ-GAN downsamples resolutions by 16x, e.g. a 256x256 (512x512) resolution image is reduced to 16x16 (32x32) latent codes. We trained our VQ-GAN for 2.5M steps.

Text Conditioning Due to our focus on inference speed, we decided to condition our model on text embeddings from a smaller CLIP model (Radford et al. (2021)) instead of T5-XXL (Raffel et al. (2023)). We experimented with both the original CLIP-l/14 (Radford et al. (2021)) and the equivalently sized CLIP model released with DataComp (Gadre et al. (2023)). Even with the reported improvements in Gadre et al. (2023), we found that the original CLIP-l/14 resulted in qualitatively better images. The penultimate text encoder hidden states are injected via the standard cross-attention mechanism. Additionally, the final pooled text encoder hidden states are injected via adaptive normalization layers (Perez et al. (2017)).

U-ViT For the base model, we used a variant of the U-ViT (Hoogeboom et al. (2023)), a transformer (Vaswani et al. (2023)) inspired scalable U-Net (Ronneberger et al. (2015)). Hoogeboom et al. (2023) finds that U-Nets can be effectively scaled by increasing the number of low-resolution blocks as the increased parameters are more than compensated for by the small feature maps. Additionally, Hoogeboom et al. (2023) turns the lowest resolution blocks into a transformer by replacing convolution blocks with MLPs. For our 256x256 resolution model, we used no downsampling or upsampling in the convolutional residual blocks. For our 512x512 resolution model, we used a single 2x downsampling and corresponding 2x upsampling in the convolutional residual blocks. As a result, the lower resolution U-ViT of the 256x256 and 512x512 models receive an input vector sequence of 256 (16x16) with a feature dimension of 1024. The 256x256 resolution model has 603M parameters, and the 512x512 resolution model has 608M parameters. The 5M additional parameters in the 512x512 resolution model are due to the additional down and upsampling layers.

Masking Schedule Following MUSE (Chang et al. (2023)) and MaskGIT (Chang et al. (2022)), we use a cosine based masking schedule. After each step t , of predicted tokens, those with the most confident predictions are permanently unmasked such that the proportion of tokens masked is $\cos(\frac{t}{T} \cdot \frac{\pi}{2})$, with T being the total number of sampling steps. We use $T = 12$ sampling steps in all of our evaluation experiments. Through ablations, Chang et al. (2022) shows that concave masking schedules like cosine outperform convex masking schedules. Chang et al. (2022) hypothesizes that

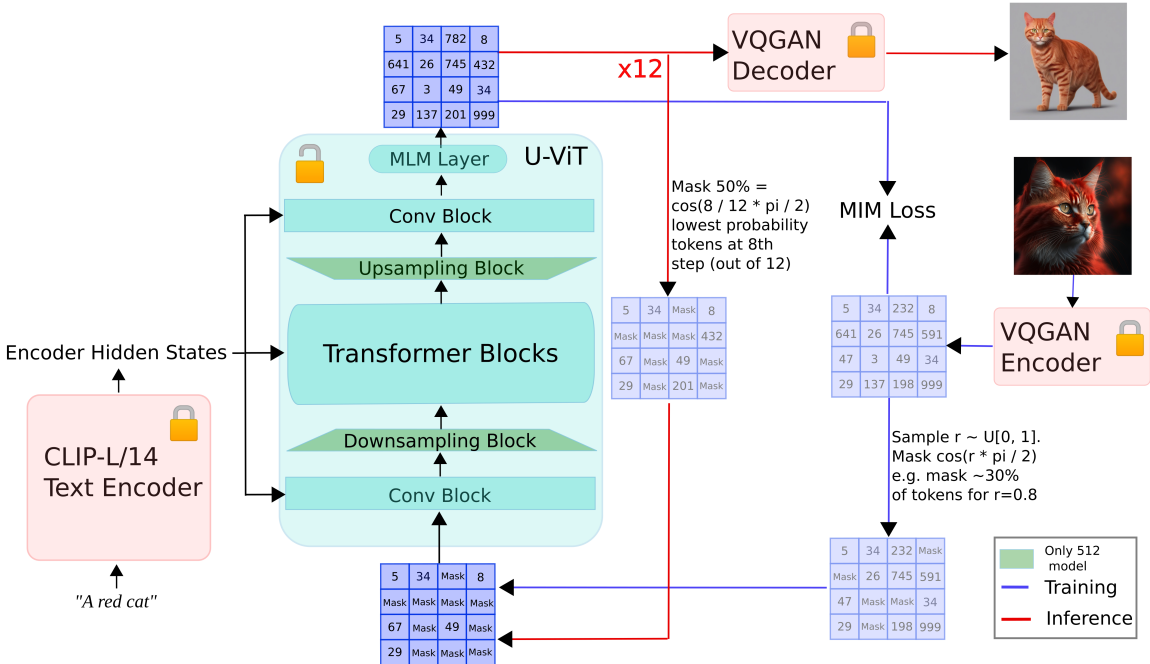


Figure 1: The diagram shows the training and inference pipelines for aMUSEd. aMUSEd consists of three separately trained components: a pre-trained CLIP-L/14 text encoder, a VQ-GAN, and a U-ViT. During training, the VQ-GAN encoder maps images to a 16x smaller latent resolution. The proportion of masked latent tokens is sampled from a cosine masking schedule, e.g. $\cos(r \cdot \frac{\pi}{2})$ with $r \sim \text{Uniform}(0, 1)$. The model is trained via cross-entropy loss to predict the masked tokens. After the model is trained on 256x256 images, downsampling and upsampling layers are added, and training is continued on 512x512 images. During inference, the U-ViT is conditioned on the text encoder’s hidden states and iteratively predicts values for all masked tokens. The cosine masking schedule determines a percentage of the most confident token predictions to be fixed after every iteration. After 12 iterations, all tokens have been predicted and are decoded by the VQ-GAN into image pixels.

concave masking schedules benefit from fewer fixed predictions earlier in the denoising process and more fixed predictions later in the denoising process.

Micro-conditioning Just as Podell et al. (2023), we micro-condition on the original image resolution, crop coordinates, and LAION aesthetic score (Schuhmann (2022)). The micro-conditioning values are projected to sinusoidal embeddings and appended as additional channels to the final pooled text encoder hidden states.

4 EXPERIMENTAL SETUP

4.1 PRE-TRAINING

Data Preparation We pre-trained on deduplicated LAION-2B (Schuhmann et al. (2022a)) with images above a 4.5 aesthetic score (Schuhmann (2022)). We filtered out images above a 50% watermark probability or above a 45% NSFW probability. The deduplicated LAION dataset was provided by Laurençon et al. (2023) using the strategy presented in Webster et al. (2023).

Training Details For pre-training, the VQ-GAN and text encoder weights were frozen, and only the U-ViTs of the respective models were trained. The 256x256 resolution model² was trained on 2

²<https://huggingface.co/amused/amused-256>

8xA100 servers for 1,000,000 steps and used a per GPU batch size of 128 for a total batch size of 2,048. The 512x512 resolution model³ was initialized from step 84,000 of the 256x256 resolution model and continued to train for 554,000 steps on 2 8xA100 servers. The 512x512 resolution model used a per GPU batch size 64 for a total batch size of 1024.

Masking Rate Sampling Following Chang et al. (2022) and Chang et al. (2023), the percentage of masked latent tokens was sampled from a cosine masking schedule, e.g. $\cos(r \cdot \frac{\pi}{2})$ with $r \sim \text{Uniform}(0, 1)$. Chang et al. (2022) ablates different choices of masking schedules, finding that concave functions outperform convex functions. They hypothesize that this is due to more challenging masking ratios during training.

4.2 FINE-TUNING

We further fine-tuned the 256x256 resolution model for 80,000 steps on journeydb (Sun et al. (2023)). We also further fine-tuned the 512x512 model for 2,000 steps on journeydb, synthetic images generated by SDXL (Podell et al. (2023)) from LAION-COCO captions (Schuhmann et al. (2022b)), unsplash lite, and LAION-2B above a 6 aesthetic score (Schuhmann et al. (2022a); Schuhmann (2022)). We found that the synthetic image generated by SDXL (Podell et al. (2023)) from LAION-COCO captions (Schuhmann et al. (2022b)) qualitatively improved text-image alignment. The 512x512 resolution model was fine-tuned for much fewer steps than the 256x256 model because it began to overfit on the fine-tuning data.

To improve the reconstruction of high-resolution images, we further fine-tuned the VQ-GAN decoder on a dataset of images greater than 1024x1024 resolution. The VQ-GAN decoder was fine-tuned on 2 8xA100 servers for 200,000 steps and used a per GPU batch size of 16 for a total batch size of 256.

5 RESULTS

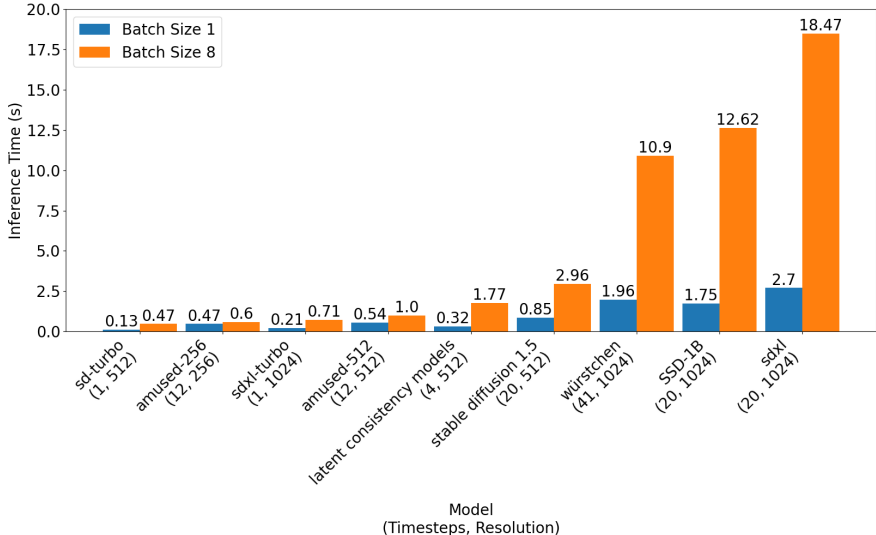


Figure 2: A100 40GB end to end image generation time. Full A100 and 4090 benchmarks can be found in appendix A.

5.1 INFERENCE SPEED

aMUSEd’s inference speed is superior to non-distilled diffusion models and competitive with few-step distilled diffusion models. Compared to many popular diffusion models, aMUSEd scales par-

³<https://huggingface.co/amused/amused-512>

ticularly well with batch size, making it a good choice for text-to-image applications that require high throughput⁴.

For batch size 1, single-step distilled diffusion models such as sd-turbo and sdxl-turbo (Sauer et al. (2023)) outperform both of our 256x256 and 512x512 resolution models. Notably, sd-turbo generates higher resolution images than our 256x256 resolution model while being 3.5x faster.

Compared to batch size 1, the end to end generation time for batch size 8 of sd-turbo (sdxl-turbo) is reduced by 3.6x (3.38x). However, aMUSED’s 256x256 (512x12) resolution model’s inference time only decreases by 1.28x (1.8x). At batch size 8, sd-turbo is still the fastest image generation model, but it is only 1.3x faster than our 256x256 resolution model. At batch size 8, aMUSED’s 256x256 (512x512) resolution model outperforms the 4-step latent consistency model by a factor of 3x (1.8x).

Both aMUSED models are significantly faster than non-distilled diffusion models. Compared to stable diffusion 1.5⁵ (Rombach et al. (2022)), the 512x512 resolution aMUSED model is 1.6x (3x) faster at batch size 1 (batch size 8). At batch size 8, the state of the art SDXL (Podell et al. (2023)) is orders of magnitude slower than both aMUSED models.

5.2 MODEL QUALITY

We benchmarked both aMUSED models on zero-shot FID (Heusel et al. (2017)), CLIP (Radford et al. (2021)), and inception score (Salimans et al. (2016)) on the MSCOCO (Lin et al. (2015)) 2017 validation set with 2 samples per caption for a total of 10k samples. Due to either a lack of reported metrics or ambiguities in measurement methodologies, we manually ran quality benchmarks for all models we compared against. Our 512x512 resolution model has competitive CLIP scores. However, both our 256x256 and 512x512 resolution models lag behind in FID and Inception scores. Subjectively, both models perform well at low detail images with few subjects, such as landscapes. Both models may perform well for highly detailed images such as faces or those with many subjects but require prompting and cherry-picking. See 3.

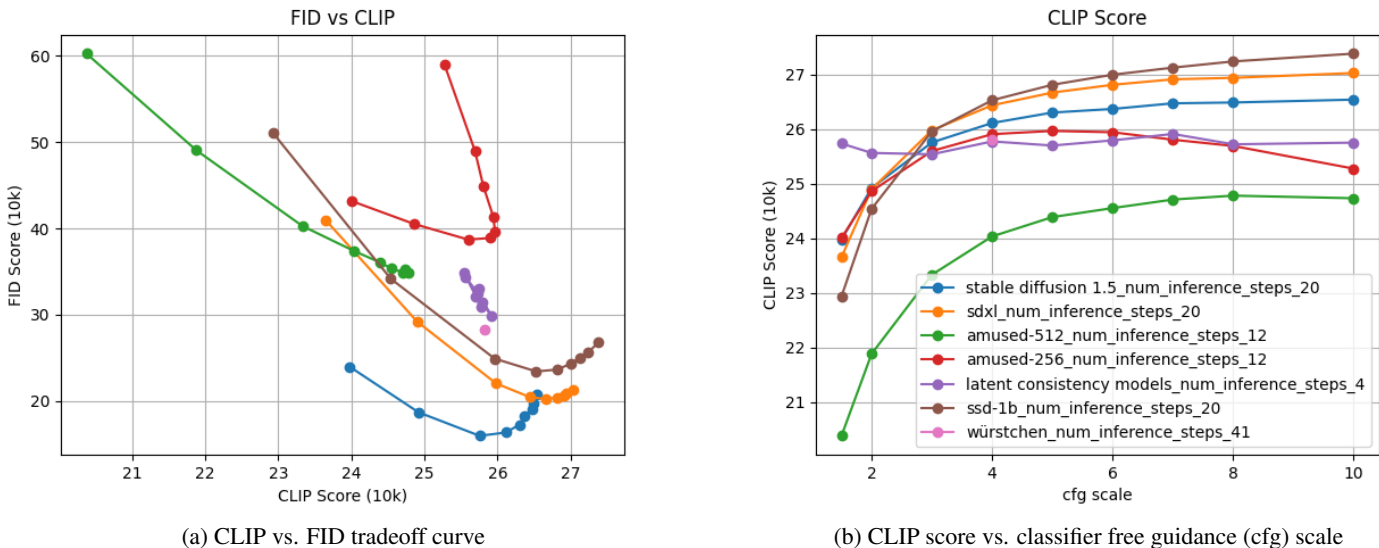


Figure 4: See appendix B for additional FID, CLIP, and inception score measurements.

⁴batch size × latency
⁵Stable diffusion 1.5 outputs images at the same 512x512 resolution as the 512x512 resolution aMUSED model.



Figure 3: Cherry-picked images from 512x512 and 256x256 resolution models. Images are slightly degraded for file size considerations

5.3 STYLEDROP

Stylerdrop (Sohn et al. (2023)) is an efficient fine-tuning method for learning a new style from a small number of images. It has an optional first stage to generate additional training samples, which can be used to augment the training dataset. Stylerdrop demonstrates effective single example image style adoption on MUSE and aMUSEd. Sohn et al. (2023) shows that similar fine-tuning procedures such as LoRa Dreambooth (Ruiz et al. (2023)) on Stable Diffusion (Rombach et al. (2022)) and Dreambooth on Imagen (Saharia et al. (2022)) do not show the same degree of style adherence. Figure 5 compares a LoRa Dreambooth Stable Diffusion training run⁶ with a stylerdrop training run on aMUSEd. Using the same reference training image and example prompts, stylerdrop on aMUSEd demonstrates much stronger style adherence. In our experiments with aMUSEd, we achieved good results with fine-tuning on a single image and not generating any additional training samples. Style-drop can cheaply fine-tune aMUSEd in as few as 1500-2000 training steps.

⁶Using the same training parameters as Sohn et al. (2023) - 400 training steps, UNet LR 2e-4, CLIP LR 5e-6



Figure 5

Model	Learning Rate	Batch Size	Memory Required	Steps	LoRa Alpha	LoRa Rank
amused-256	4e-4	1	6.5 GB	1500-2000	32	16
amused-512	1e-3	1	5.6 GB	1500-2000	1	16

Table 1: Styledrop configs. LoRa applied to all QKV projections.

5.4 8BIT QUANTIZATION

Token based modeling allows for the use of techniques from the language modeling literature, such as 8-bit quantization for transformer feed-forward and attention projection layers (Dettmers et al. (2022)). Using 8-bit quantization, we can load the whole model with as little as 800 MB of VRAM, making mobile and CPU applications more feasible.



Figure 6: aMUSEd 256x256 images with 8-bit quantization

5.5 TASK TRANSFER

Image variation and in-painting Similar to Chang et al. (2023), aMUSEd performs zero-shot image editing tasks such as image variation and in-painting. For masked token based image modeling, both image variation and in-painting are close to the default training objective, so both tasks use

the regular decoding procedure. For image variation, some number of latent tokens are masked with more masked latent tokens corresponding to more variation from the original image. For in-painting, the in-painting mask directly determines which tokens are initially masked.

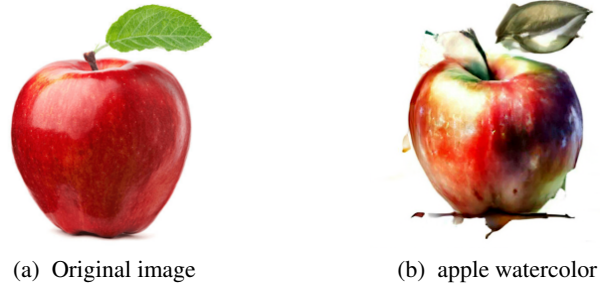


Figure 7: aMUSEd 256x256 image variation

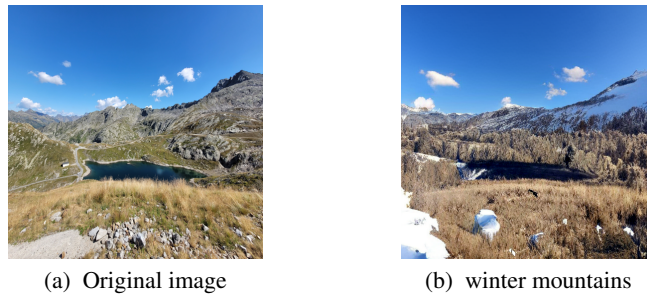


Figure 8: aMUSEd 512x512 image variation

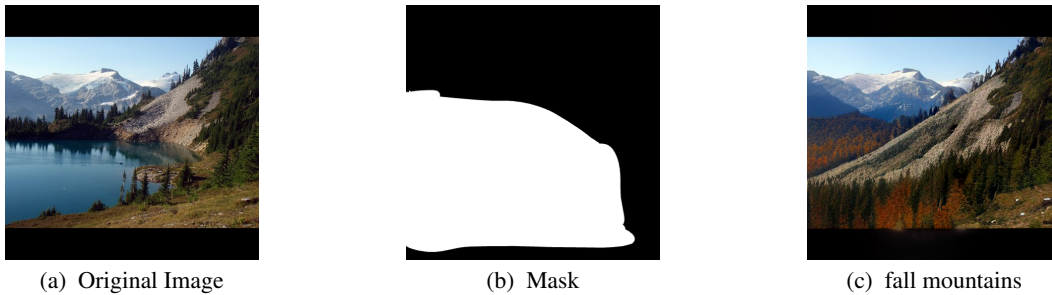


Figure 9: aMUSEd 512x512 in-painting

Video generation We further extended aMUSEd to zero-shot video generation by modifying text2video-zero (Khachatryan et al. (2023)). Text2video-zero operates on stable diffusion’s (Rom-bach et al. (2022)) continuous latents. Noised latents are warped by varying amounts to produce latents for successive frames. Additional noise is then added to the frame latents. During the standard denoising process, self attention is replaced with cross-attention over the first frame to maintain temporal consistency. Because aMUSEd operates on quantized latents, we must first de-quantize the latents before they are warped. We can then re-quantize the warped latents. Because the aMUSEd latent space is discrete, we completely re-mask the boundary of the image warp, which creates consistent image backgrounds from frame to frame. We found that the between-frame cross-attention degraded quality for frames warped too far away from the initial frame, so we did not use the modified self attention and instead performed the warp much later in the denoising process.

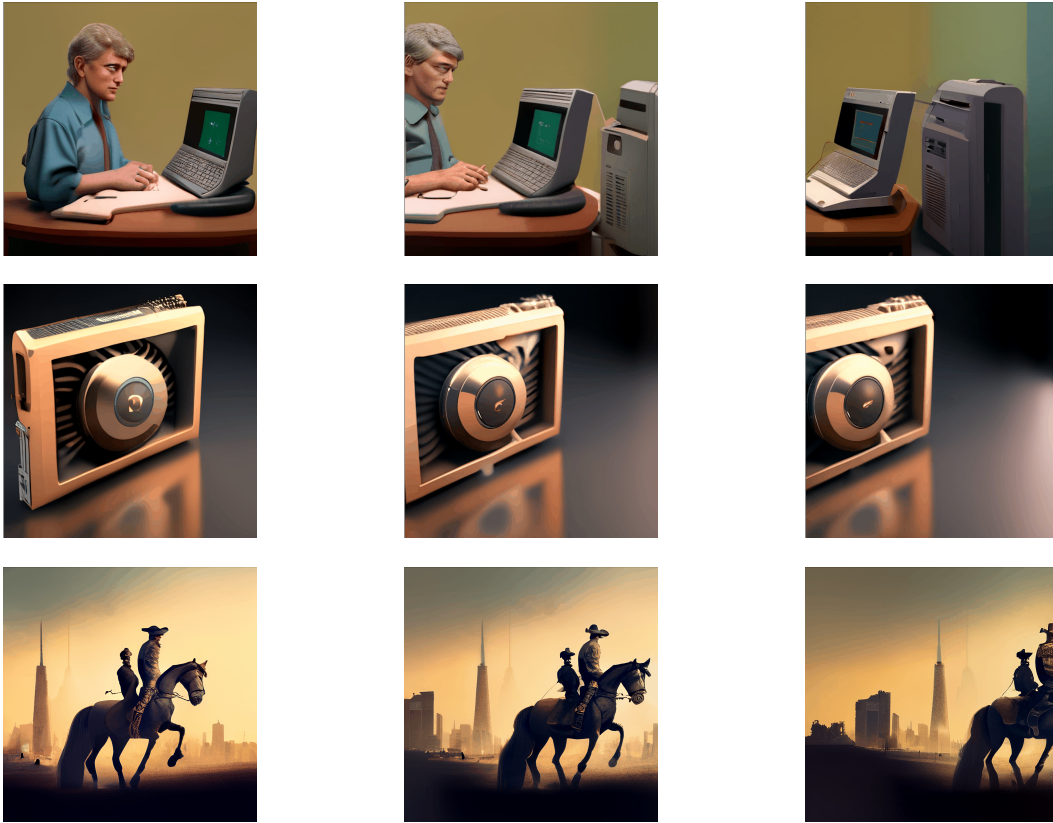


Figure 10: Video generation examples. Full videos

6 ETHICS AND SAFETY

We filtered out images in the training data above a 50% watermark probability or above a 45% NSFW probability. We manually checked that both models do not accurately follow NSFW prompts and therefore concluded that our NSFW filtering helps prevent possible harmful use cases.

7 CONCLUSION

We introduced aMUSEd, a lightweight and open-source reproduction of MUSE. Our primary goal was to achieve fast sampling and provide an efficient alternative to diffusion models. In our reproduction, aMUSEd demonstrated competitive zero-shot image variation and in-painting without requiring task specific training. We made several modifications for efficiency, including the use of the smaller CLIP-l/14 text encoder (Radford et al. (2021)) and an efficient U-ViT (Hoogeboom et al. (2023)) backbone. Our results show that aMUSEd’s inference speed is competitive with distilled diffusion-based text-to-image models, particularly when scaling with batch size. Additionally, aMUSEd demonstrates efficient fine-tuning capabilities, providing flexibility for various applications. We hope that by open-sourcing all model weights and code, future research into masked image modeling for text-to-image generation is made more accessible.

8 CONTRIBUTION & ACKNOWLEDGEMENT

Suraj led training. William led data and supported training. Patrick supported both training and data and provided general guidance. Robin trained the VQ-GAN and provided general guidance.

Also, immense thanks to community contributor Isamu Isozaki for helpful discussions and code contributions.

REFERENCES

- Armen Aghajanyan, Bernie Huang, Candace Ross, Vladimir Karpukhin, Hu Xu, Naman Goyal, Dmytro Okhonko, Mandar Joshi, Gargi Ghosh, Mike Lewis, et al. Cm3: A causal masked multi-modal model of the internet. *arXiv preprint arXiv:2201.07520*, 2022.
- James Betker, Gabriel Goh, Li Jing, Tim Brooks, Jianfeng Wang, Linjie Li, Long Ouyang, Juntang Zhuang, Joyce Lee, Yufei Guo, Wesam Manassra, Prafulla Dhariwal, Casey Chu, Yunxin Jiao, and Aditya Ramesh. Improving image generation with better captions. 2023.
- Huiwen Chang, Han Zhang, Lu Jiang, Ce Liu, and William T. Freeman. Maskgit: Masked generative image transformer, 2022.
- Huiwen Chang, Han Zhang, Jarred Barber, AJ Maschinot, Jose Lezama, Lu Jiang, Ming-Hsuan Yang, Kevin Murphy, William T. Freeman, Michael Rubinstein, Yuanzhen Li, and Dilip Krishnan. Muse: Text-to-image generation via masked generative transformers, 2023.
- Junsong Chen, Jincheng Yu, Chongjian Ge, Lewei Yao, Enze Xie, Yue Wu, Zhongdao Wang, James Kwok, Ping Luo, Huchuan Lu, et al. Pixart- α : Fast training of diffusion transformer for photorealistic text-to-image synthesis. *arXiv preprint arXiv:2310.00426*, 2023.
- DeepFloyd. Stability ai releases deepfloyd if, a powerful text-to-image model that can smartly integrate text into images. <https://stability.ai/news/deepfloyd-if-text-to-image-model>, 2023.
- Tim Dettmers, Mike Lewis, Younes Belkada, and Luke Zettlemoyer. Llm.int8(): 8-bit matrix multiplication for transformers at scale, 2022.
- Tim Dettmers, Artidoro Pagnoni, Ari Holtzman, and Luke Zettlemoyer. Qlora: Efficient finetuning of quantized llms, 2023.
- Jacob Devlin, Ming-Wei Chang, Kenton Lee, and Kristina Toutanova. Bert: Pre-training of deep bidirectional transformers for language understanding. *arXiv preprint arXiv:1810.04805*, 2018.
- Tim Dockhorn, Arash Vahdat, and Karsten Kreis. Genie: Higher-order denoising diffusion solvers, 2022.
- Patrick Esser, Robin Rombach, and Björn Ommer. Taming transformers for high-resolution image synthesis, 2021.
- Angela Fan, Mike Lewis, and Yann Dauphin. Hierarchical neural story generation, 2018.
- Samir Yitzhak Gadre, Gabriel Ilharco, Alex Fang, Jonathan Hayase, Georgios Smyrnis, Thao Nguyen, Ryan Marten, Mitchell Wortsman, Dhruva Ghosh, Jieyu Zhang, Eyal Orgad, Rahim Entezari, Giannis Daras, Sarah Pratt, Vivek Ramanujan, Yonatan Bitton, Kalyani Marathe, Stephen Mussmann, Richard Vencu, Mehdi Cherti, Ranjay Krishna, Pang Wei Koh, Olga Saukh, Alexander Ratner, Shuran Song, Hannaneh Hajishirzi, Ali Farhadi, Romain Beaumont, Sewoong Oh, Alex Dimakis, Jenia Jitsev, Yair Carmon, Vaishaal Shankar, and Ludwig Schmidt. Datacomp: In search of the next generation of multimodal datasets, 2023.
- Chuan Guo, Geoff Pleiss, Yu Sun, and Kilian Q. Weinberger. On calibration of modern neural networks, 2017.
- Martin Heusel, Hubert Ramsauer, Thomas Unterthiner, Bernhard Nessler, and Sepp Hochreiter. Gans trained by a two time-scale update rule converge to a local nash equilibrium. *Advances in neural information processing systems*, 30, 2017.
- Ari Holtzman, Jan Buys, Li Du, Maxwell Forbes, and Yejin Choi. The curious case of neural text degeneration, 2020.
- Emiel Hoogeboom, Jonathan Heek, and Tim Salimans. Simple diffusion: End-to-end diffusion for high resolution images, 2023.
- Edward J. Hu, Yelong Shen, Phillip Wallis, Zeyuan Allen-Zhu, Yuanzhi Li, Shean Wang, Lu Wang, and Weizhu Chen. Lora: Low-rank adaptation of large language models, 2021.

- Shaohan Huang, Li Dong, Wenhui Wang, Yaru Hao, Saksham Singhal, Shuming Ma, Tengchao Lv, Lei Cui, Owais Khan Mohammed, Qiang Liu, et al. Language is not all you need: Aligning perception with language models. *arXiv preprint arXiv:2302.14045*, 2023.
- Zhengbao Jiang, Jun Araki, Haibo Ding, and Graham Neubig. How can we know when language models know? on the calibration of language models for question answering. *Transactions of the Association for Computational Linguistics*, 9:962–977, 2021. doi: 10.1162/tacl_a.00407. URL <https://aclanthology.org/2021.tacl-1.57>.
- Tero Karras, Miika Aittala, Timo Aila, and Samuli Laine. Elucidating the design space of diffusion-based generative models. *Advances in Neural Information Processing Systems*, 35:26565–26577, 2022.
- Levon Khachatryan, Andranik Movsisyan, Vahram Tadevosyan, Roberto Henschel, Zhangyang Wang, Shant Navasardyan, and Humphrey Shi. Text2video-zero: Text-to-image diffusion models are zero-shot video generators, 2023.
- Diederik P. Kingma and Max Welling. An introduction to variational autoencoders. *CoRR*, abs/1906.02691, 2019. URL <http://arxiv.org/abs/1906.02691>.
- Hugo Laurençon, Lucile Saulnier, Léo Tronchon, Stas Bekman, Amanpreet Singh, Anton Lozhkov, Thomas Wang, Siddharth Karamcheti, Alexander M. Rush, Douwe Kiela, Matthieu Cord, and Victor Sanh. Obelics: An open web-scale filtered dataset of interleaved image-text documents, 2023.
- Tsung-Yi Lin, Michael Maire, Serge Belongie, Lubomir Bourdev, Ross Girshick, James Hays, Pietro Perona, Deva Ramanan, C. Lawrence Zitnick, and Piotr Dollár. Microsoft coco: Common objects in context, 2015.
- Cheng Lu, Yuhao Zhou, Fan Bao, Jianfei Chen, Chongxuan Li, and Jun Zhu. Dpm-solver: A fast ode solver for diffusion probabilistic model sampling in around 10 steps. *arXiv preprint arXiv:2206.00927*, 2022a.
- Cheng Lu, Yuhao Zhou, Fan Bao, Jianfei Chen, Chongxuan Li, and Jun Zhu. Dpm-solver++: Fast solver for guided sampling of diffusion probabilistic models. *arXiv preprint arXiv:2211.01095*, 2022b.
- Simian Luo, Yiqin Tan, Longbo Huang, Jian Li, and Hang Zhao. Latent consistency models: Synthesizing high-resolution images with few-step inference, 2023a.
- Simian Luo, Yiqin Tan, Suraj Patil, Daniel Gu, Patrick von Platen, Apolinário Passos, Longbo Huang, Jian Li, and Hang Zhao. Lcm-lora: A universal stable-diffusion acceleration module, 2023b.
- William Peebles and Saining Xie. Scalable diffusion models with transformers, 2023.
- Ethan Perez, Florian Strub, Harm de Vries, Vincent Dumoulin, and Aaron Courville. Film: Visual reasoning with a general conditioning layer, 2017.
- Dustin Podell, Zion English, Kyle Lacey, Andreas Blattmann, Tim Dockhorn, Jonas Müller, Joe Penna, and Robin Rombach. Sdxl: improving latent diffusion models for high-resolution image synthesis. *arXiv preprint arXiv:2307.01952*, 2023.
- Ben Poole, Ajay Jain, Jonathan T. Barron, and Ben Mildenhall. Dreamfusion: Text-to-3d using 2d diffusion, 2022.
- Alec Radford, Jong Wook Kim, Chris Hallacy, Aditya Ramesh, Gabriel Goh, Sandhini Agarwal, Girish Sastry, Amanda Askell, Pamela Mishkin, Jack Clark, et al. Learning transferable visual models from natural language supervision. In *International conference on machine learning*, pp. 8748–8763. PMLR, 2021.
- Colin Raffel, Noam Shazeer, Adam Roberts, Katherine Lee, Sharan Narang, Michael Matena, Yanqi Zhou, Wei Li, and Peter J. Liu. Exploring the limits of transfer learning with a unified text-to-text transformer, 2023.

- Aditya Ramesh, Mikhail Pavlov, Gabriel Goh, Scott Gray, Chelsea Voss, Alec Radford, Mark Chen, and Ilya Sutskever. Zero-shot text-to-image generation, 2021.
- Aditya Ramesh, Prafulla Dhariwal, Alex Nichol, Casey Chu, and Mark Chen. Hierarchical text-conditional image generation with clip latents. *arXiv preprint arXiv:2204.06125*, 2022.
- Robin Rombach, Andreas Blattmann, Dominik Lorenz, Patrick Esser, and Björn Ommer. High-resolution image synthesis with latent diffusion models. In *Proceedings of the IEEE/CVF Conference on Computer Vision and Pattern Recognition*, pp. 10684–10695, 2022.
- Olaf Ronneberger, Philipp Fischer, and Thomas Brox. U-net: Convolutional networks for biomedical image segmentation, 2015.
- Nataniel Ruiz, Yuanzhen Li, Varun Jampani, Yael Pritch, Michael Rubinstein, and Kfir Aberman. Dreambooth: Fine tuning text-to-image diffusion models for subject-driven generation, 2023.
- RunwayML. Stable diffusion inpainting. <https://huggingface.co/runwayml/stable-diffusion-inpainting>, 2022.
- Chitwan Saharia, William Chan, Saurabh Saxena, Lala Li, Jay Whang, Emily Denton, Seyed Kammar Seyed Ghasemipour, Burcu Karagol Ayan, S. Sara Mahdavi, Rapha Gontijo Lopes, Tim Salimans, Jonathan Ho, David J Fleet, and Mohammad Norouzi. Photorealistic text-to-image diffusion models with deep language understanding, 2022.
- Tim Salimans and Jonathan Ho. Progressive distillation for fast sampling of diffusion models. *arXiv preprint arXiv:2202.00512*, 2022.
- Tim Salimans, Ian Goodfellow, Wojciech Zaremba, Vicki Cheung, Alec Radford, and Xi Chen. Improved techniques for training gans, 2016.
- Axel Sauer, Dominik Lorenz, Andreas Blattmann, and Robin Rombach. Adversarial diffusion distillation, 2023.
- Christoph Schuhmann. Laion-aesthetics. <https://laion.ai/blog/laion-aesthetics/>, 2022.
- Christoph Schuhmann, Romain Beaumont, Richard Vencu, Cade Gordon, Ross Wightman, Mehdi Cherti, Theo Coombes, Aarush Katta, Clayton Mullis, Mitchell Wortsman, et al. Laion-5b: An open large-scale dataset for training next generation image-text models. *arXiv preprint arXiv:2210.08402*, 2022a.
- Christoph Schuhmann, Andreas Köpf, Richard Vencu, Theo Coombes, and Romain Beaumont. Laion coco: 600m synthetic captions from laion2b-en. <https://laion.ai/blog/laion-coco/>, 2022b.
- Kihyuk Sohn, Nataniel Ruiz, Kimin Lee, Daniel Castro Chin, Irina Blok, Huiwen Chang, Jarred Barber, Lu Jiang, Glenn Entis, Yuanzhen Li, Yuan Hao, Irfan Essa, Michael Rubinstein, and Dilip Krishnan. Styledrop: Text-to-image generation in any style, 2023.
- Jiaming Song, Chenlin Meng, and Stefano Ermon. Denoising diffusion implicit models. *arXiv preprint arXiv:2010.02502*, 2020.
- Yang Song, Jascha Sohl-Dickstein, Diederik P. Kingma, Abhishek Kumar, Stefano Ermon, and Ben Poole. Score-based generative modeling through stochastic differential equations, 2021.
- Keqiang Sun, Juntong Pan, Yuying Ge, Hao Li, Haodong Duan, Xiaoshi Wu, Renrui Zhang, Aojun Zhou, Zipeng Qin, Yi Wang, Jifeng Dai, Yu Qiao, Limin Wang, and Hongsheng Li. Journeydb: A benchmark for generative image understanding, 2023.
- Ashish Vaswani, Noam Shazeer, Niki Parmar, Jakob Uszkoreit, Llion Jones, Aidan N. Gomez, Lukasz Kaiser, and Illia Polosukhin. Attention is all you need, 2023.
- Patrick von Platen, Suraj Patil, Anton Lozhkov, Pedro Cuenca, Nathan Lambert, Kashif Rasul, Mishig Davaadorj, and Thomas Wolf. Diffusers: State-of-the-art diffusion models. URL <https://github.com/huggingface/diffusers>.

- Ryan Webster, Julien Rabin, Loic Simon, and Frederic Jurie. On the de-duplication of laion-2b, 2023.
- Jiahui Yu, Yuanzhong Xu, Jing Yu Koh, Thang Luong, Gunjan Baid, Zirui Wang, Vijay Vasudevan, Alexander Ku, Yinfei Yang, Burcu Karagol Ayan, Ben Hutchinson, Wei Han, Zarana Parekh, Xin Li, Han Zhang, Jason Baldridge, and Yonghui Wu. Scaling autoregressive models for content-rich text-to-image generation, 2022.
- Lili Yu, Bowen Shi, Ramakanth Pasunuru, Benjamin Muller, Olga Golovneva, Tianlu Wang, Arun Babu, Binh Tang, Brian Karrer, Shelly Sheynin, Candace Ross, Adam Polyak, Russell Howes, Vasu Sharma, Puxin Xu, Hovhannes Tamoyan, Oron Ashual, Uriel Singer, Shang-Wen Li, Susan Zhang, Richard James, Gargi Ghosh, Yaniv Taigman, Maryam Fazel-Zarandi, Asli Celikyilmaz, Luke Zettlemoyer, and Armen Aghajanyan. Scaling autoregressive multi-modal models: Pretraining and instruction tuning, 2023.
- Qinsheng Zhang and Yongxin Chen. Fast sampling of diffusion models with exponential integrator, 2023.
- Wenliang Zhao, Lujia Bai, Yongming Rao, Jie Zhou, and Jiwen Lu. Unipc: A unified predictor-corrector framework for fast sampling of diffusion models. *arXiv preprint arXiv:2302.04867*, 2023.
- Kaiwen Zheng, Cheng Lu, Jianfei Chen, and Jun Zhu. Dpm-solver-v3: Improved diffusion ode solver with empirical model statistics, 2023.

A INFERENCE SPEED

All measurements were taken in fp16 with the diffusers library (von Platen et al.) model implementations. All measurements are of end to end image generation.

Model	inference time	timesteps	resolution	Model	inference time	timesteps	resolution
sd-turbo	0.13 s	1	512	sd-turbo	0.47 s	1	512
sdxl-turbo	0.21 s	1	1024	amused-256	0.6 s	12	256
latent consistency models	0.32 s	4	512	sdxl-turbo	0.71 s	1	1024
amused-256	0.47 s	12	256	amused-512	1.0 s	12	512
amused-512	0.54 s	12	512	latent consistency models	1.77 s	4	512
stable diffusion 1.5	0.85 s	20	512	stable diffusion 1.5	2.96 s	20	512
SSD-1B	1.75 s	20	1024	würstchen	10.9 s	41	1024
würstchen	1.96 s	41	1024	SSD-1B	12.62 s	20	1024
sdxl	2.7 s	20	1024	sdxl	18.47 s	20	1024

(a) batch size 1

(b) batch size 8

Figure 11: A100 inference time measurements

Model	inference time	timesteps	resolution	Model	inference time	timesteps	resolution
sd-turbo	0.07 s	1	512	sd-turbo	0.44 s	1	512
sdxl-turbo	0.11 s	1	1024	amused-256	0.45 s	12	256
amused-256	0.2 s	12	256	sdxl-turbo	0.75 s	1	1024
latent consistency models	0.24 s	4	512	amused-512	0.76 s	12	512
amused-512	0.24 s	12	512	latent consistency models	1.61 s	4	512
stable diffusion 1.5	0.55 s	20	512	stable diffusion 1.5	3.16 s	20	512
würstchen	1.34 s	41	1024	würstchen	11.15 s	41	1024
SSD-1B	1.88 s	20	1024	SSD-1B	11.73 s	20	1024
sdxl	2.84 s	20	1024	sdxl	18.38 s	20	1024

(a) batch size 1

(b) batch size 8

Figure 12: 4090 inference time measurements

B MODEL QUALITY

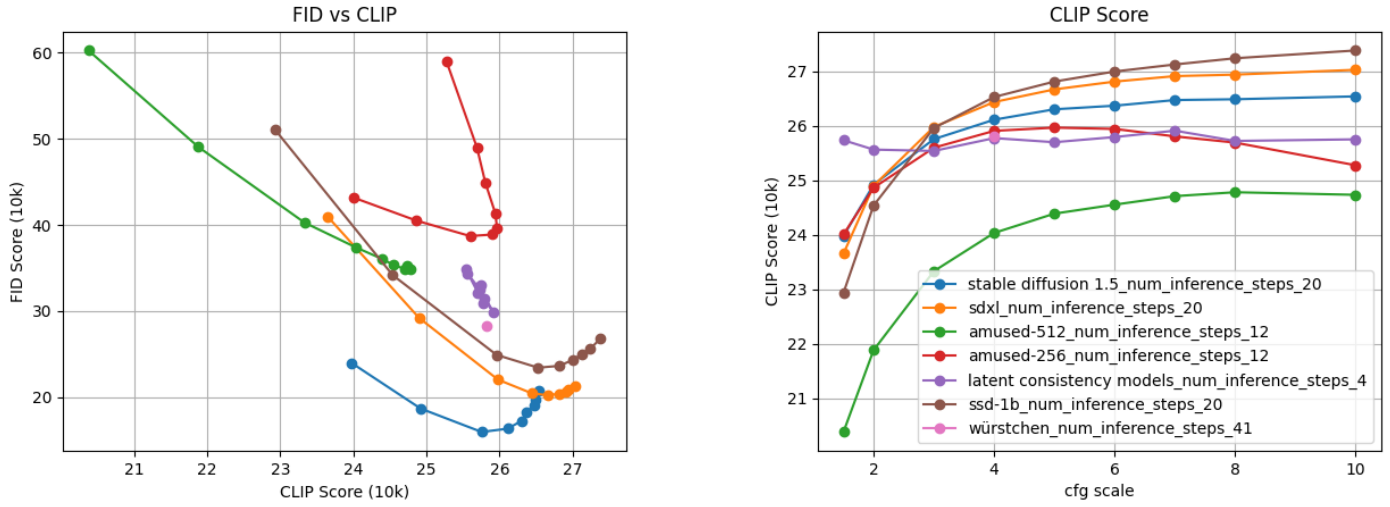


Figure 13

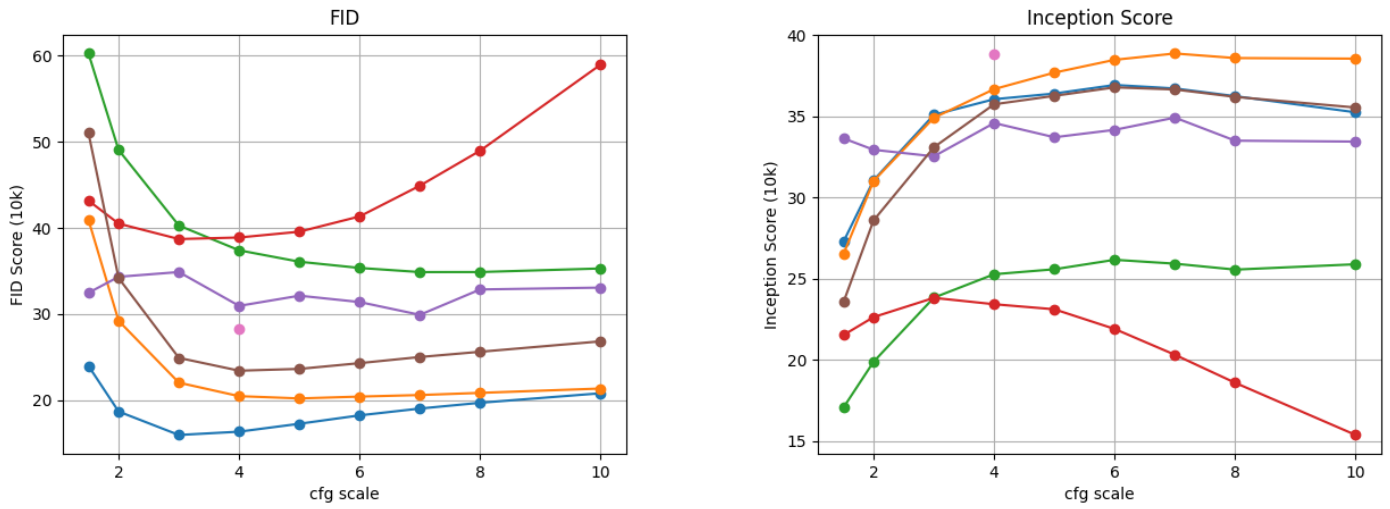


Figure 14

Model	CLIP	guidance scale	timesteps	resolution
ssd-1b	27.38	10.0	20	1024
sdxl	27.03	10.0	20	1024
stable diffusion 1.5	26.54	10.0	20	512
amused-256	25.97	5.0	12	256
latent consistency models	25.91	7.0	4	512
würstchen	25.82	4.0	41	1024x1536
amused-512	24.78	8.0	12	512

(a) CLIP

Model	FID	guidance scale	timesteps	resolution
stable diffusion 1.5	15.97	3.0	20	512
sdxl	20.21	5.0	20	1024
ssd-1b	23.43	4.0	20	1024
würstchen	28.28	4.0	41	1024x1536
latent consistency models	29.91	7.0	4	512
amused-512	34.87	7.0	12	512
amused-256	38.7	3.0	12	256

(b) FID

Model	ISC	guidance scale	timesteps	resolution
sdxl	38.88	7.0	20	1024
würstchen	38.82	4.0	41	1024x1536
stable diffusion 1.5	36.94	6.0	20	512
ssd-1b	36.79	6.0	20	1024
latent consistency models	34.93	7.0	4	512
amused-512	26.16	6.0	12	512
amused-256	23.82	3.0	12	256

(c) Inception Score

Figure 15: Model Quality Tables

C FINETUNING

aMUSEd can be finetuned on simple datasets relatively cheaply and quickly. Using LoRa (Hu et al. (2021)), and gradient accumulation, aMUSEd can be finetuned with as little as 5.6 GB VRAM.

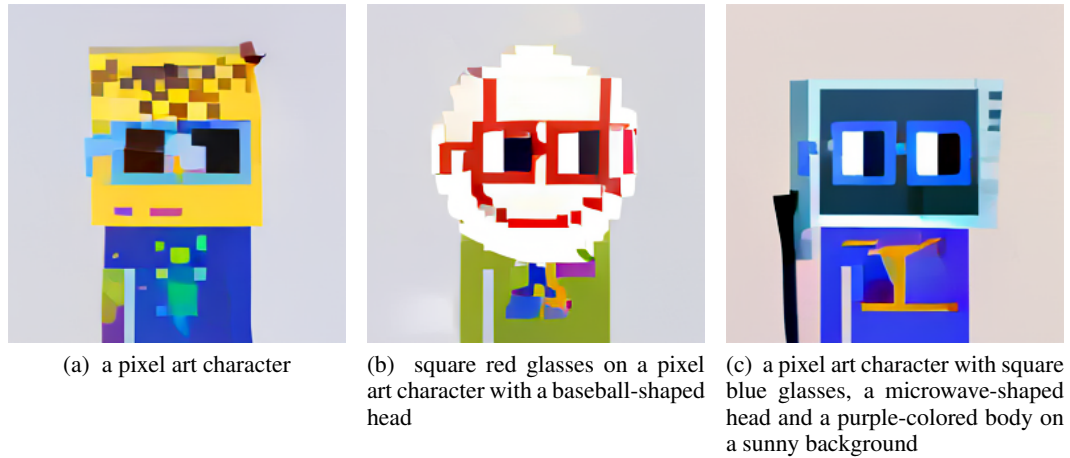


Figure 16: Example outputs of finetuning 256x256 model on dataset

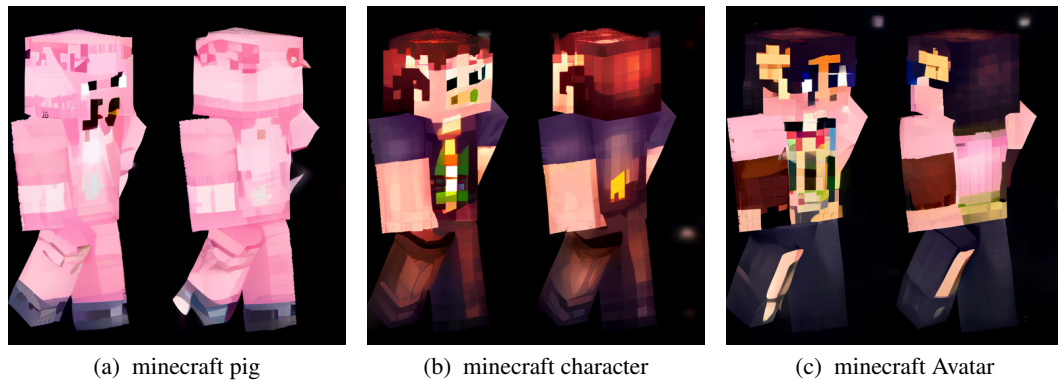


Figure 17: Example outputs of fine-tuning 512x512 model on dataset

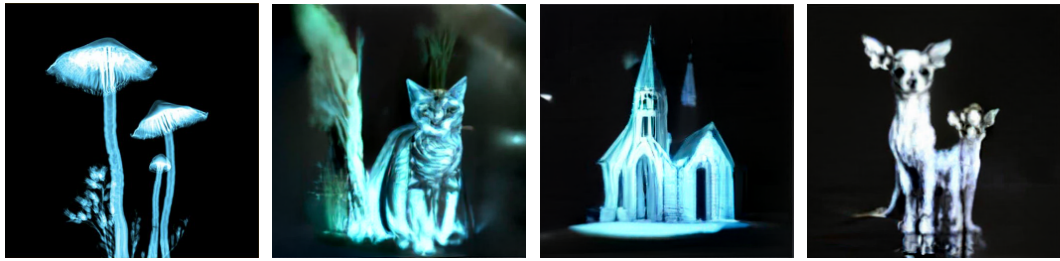
8bit Adam	LoRa	Single Step Batch Size	Grad. Accum. Steps	Learning Rate	Memory	Steps
No	No	8	1	1e-4	19.7 GB	750-1000
No	No	4	2	1e-4	18.3 GB	750-1000
No	No	1	8	1e-4	17.9 GB	750-1000
Yes	No	16	1	2e-5	20.1 GB	~ 750
Yes	No	8	2	2e-5	15.6 GB	~ 750
Yes	No	1	16	2e-5	10.7 GB	~ 750
No	Yes	16	1	8e-4	14.1 GB	1000-1250
No	Yes	8	2	8e-4	10.1 GB	1000-1250
No	Yes	1	16	8e-4	6.5 GB	1000-1250

Table 2: amused-256 fine-tuning configs. All LoRa trainings used rank 16 and alpha 32. LoRa applied to all QKV projections. dataset

8bit Adam	LoRa	Single Step Batch Size	Grad. Accum. Steps	Learning Rate	Memory	Steps
No	No	8	1	8e-5	24.2 GB	500-1000
No	No	4	2	8e-5	19.7 GB	500-1000
No	No	1	8	8e-5	16.99 GB	500-1000
Yes	No	8	1	5e-6	21.2 GB	500-1000
Yes	No	4	2	5e-6	13.3 GB	500-1000
Yes	No	1	8	5e-6	9.9 GB	500-1000
No	Yes	8	1	1e-4	12.7 GB	500-1000
No	Yes	4	2	1e-4	9.0 GB	500-1000
No	Yes	1	8	1e-4	5.6 GB	500-1000

Table 3: amused 5-12 fine-tuning configs. All LoRa trainings used rank 16 and alpha 32. LoRa applied to all QKV projections. dataset

D STYLEDROP EXAMPLES



(a) Reference image: A mushroom in [V] style (b) A tabby cat walking in the forest in [V] style (c) A church on the street in [V] style (d) A chihuahua walking on the street in [V] style

Figure 18: Styledrop amused-256



(a) Reference image: A mushroom in [V] style (b) A tabby cat walking in the forest in [V] style (c) A church on the street in [V] style (d) A chihuahua walking on the street in [V] style

Figure 19: LoRa Dreambooth Stable Diffusion



(a) Reference image: A bear in [V] style.png (b) A tabby cat walking in the forest in [V] style (c) A church on the street in [V] style (d) A chihuahua walking on the street in [V] style

Figure 20: Styledrop amused-512

Model	Learning Rate	Batch Size	Memory Required	Steps	LoRa Alpha	LoRa Rank
amused-256	4e-4	1	6.5 GB	1500-2000	32	16
amused-512	1e-3	1	5.6 GB	1500-2000	1	16

Table 4: Styledrop configs. LoRa applied to all QKV projections.